

Dual-Excitation Computer-Recursion Method of Separating Raman Scattering from Fluorescence

Y. C. Chu and G. E. Walrafen*

Chemistry Department, Howard University, Washington, D.C. 20059

Received: October 18, 1999; In Final Form: January 13, 2000

A new, two-color, e.g., 476.5 versus 488.0 nm, excitation method of recursively separating fluorescence from Raman scattering is made practical by the use of modern computers. The method is first illustrated by a three-color (476.5, 488.0, 514.5 nm) example involving the Raman spectrum from pure water, compared to the total Raman plus fluorescence spectrum from an extremely dilute, red, fluorescent dye dissolved in water. In this case the Raman spectrum from water is visible, weakly, above the more intense fluorescence background from the dye. The method is next applied using two-color excitation, only, to the much more difficult case of a highly-fluorescent, opaque, black, solid diamond composite, whose Raman scattering is obscured, entirely, by intense fluorescence. The total experimental spectrum is dominated by the fluorescence contribution, but the pure Raman spectrum, when finally separated by computation using recursion equations, shows a broad, single peak from diamond, centered at 1330 cm^{-1} , in agreement with the sample's composition, as determined by X-ray diffraction. A second diamond-composite example involves a highly-fluorescent solid composed of diamond and graphite, where Raman peaks from diamond, as well as from graphite, $\approx 1600\text{ cm}^{-1}$, are revealed by the new computer-recursion method.

Introduction

Fluorescence is the bane of Raman spectroscopy. Much effort has been applied to the complete or partial removal of the effects of fluorescence from Raman spectra. Such effort may be divided into two categories: physical and chemical. The physical category involves such procedures as time discrimination,¹ excitation by ultraviolet laser radiation to separate the Raman scattering from the lower-energy, e.g., red, fluorescence,² excitation by red laser radiation to preclude the energy needed for the fluorescence process,³ laser bleaching,² quenching,⁴ etc. The chemical category, used mainly on gases or liquids, involves removal or treatment of the offending fluorescent impurities, such as ultrafiltration,⁵ multiple distillations in a closed system containing the Raman cell,⁶ treatment with activated carbon, followed by filtration, or passage through large charcoal filters,^{7,8} ozonation,⁹ addition of hydrogen peroxide,¹⁰ etc.

In the current approach, which falls in the physical category, we combine consecutive excitation with two laser colors, e.g., 476.5 versus 488.0 nm, or 488.0 versus 514.5 nm, etc., with recursion equations, either forward or backward, as described below, and the use of a high-speed computer to compute the Raman and fluorescence contributions, separately, which result from the total spectral intensities obtained by sequential excitation at the two different laser frequencies, and at precisely the same sample position.

Our two-color recursion-equation computation method is described in detail below.

Experimental Procedure

Spectra, namely, total fluorescence plus Raman spectra, were obtained with an Instruments S. A. U-1000 holographic grating double monochromator. Excitation was accomplished with a Spectra Physics Model 265 argon ion laser, using a power level (most frequencies) of 100 mW. The spectral slit width cor-

responded to 10 cm^{-1} in all cases, with a slit height of 1 cm. Raman geometries employed were of the $X(Z, X + Z)Y$ type. Scanning and recording were accomplished with Instruments S. A. "Prism" software and instrumentation. Detection involved a cooled RCA 31034A-02 photomultiplier tube.

Meticulous care involving a series of pin holes, etc., was taken to position the laser spot as precisely as possible on the same sample position when changing the laser frequencies. This precaution was necessary, especially in the case of the diamond-composite samples, to ensure against spatial inhomogeneity in the fluorescence, surface irregularity, etc.

Diamond-composite samples were kindly supplied to us by Professor B. Kear, of Rutgers University. Some samples were given to us by Dr. L. A. Kabacoff. X-ray diffraction analysis was provided by Dr. Kabacoff for some samples, and by Dr. G. J. Piermarini for others.

The diamond-composite samples were thoroughly cleaned with solvents such as CCl_4 , followed by a series of acids, e.g., 48 wt % HF at $70\text{ }^\circ\text{C}$ for 30 min, then by immersion in aqua regia, and finally by heating in 90 wt % sulfuric acid at $120\text{ }^\circ\text{C}$ for 30 min. However, such cleaning was found to be entirely ineffective on the fluorescence level of the samples.

The aqueous solution containing the fluorescent dye was prepared by very quickly dipping the tip of a fine, red, felt-point "Papermate" pen, containing a water soluble dye, into water. The resulting dilute solution was then further diluted with water until the desired fluorescence level, compared to the Raman scattering intensity from the pure water, was obtained. We emphasize that this procedure, and the resultant spectra, were employed solely to serve as a simple example of our procedure, for those workers not conversant in spectroscopy.

Recursion Equations

We designate the four primary argon-ion laser excitations employed here as follows: violet, 457.9 nm, *D*; blue 2, 476.5

nm, *C*; blue 1, 488.0 nm, *B*; and green, 514.5 nm, *A*. (*A* and *B* are much more intense than *C* and *D*.)

We employ the symbols T, for total; R, for Raman, and F, for fluorescence. The wavenumber shift between two excitations is designated by Δ . For example, $\Delta = 494.6 \text{ cm}^{-1}$, for $B \rightarrow C$, and $\Delta = 1055.5 \text{ cm}^{-1}$, for $A \rightarrow B$. ω is the Raman shift in cm^{-1} .

The intensity of a specific type is a function of three variables, $I(x,y,z) = I[(A,B,C,D); (T,R,F); \omega]$. For example, the pure fluorescence intensity excited by the blue 1, 488.0 nm, *B* radiation is designated as, $I(x,y,z) = I(B,F,\omega)$. Such designations are important in the recursions relations to follow.

The Raman intensity, upon changing from the *C* to *B* radiations, is given as follows,

$$I(C,R,\omega) = I(B,R,\omega)\eta \quad (1)$$

where η is an experimental factor which corrects the Raman intensity for the change from the *C* to *B* excitations, e.g., power level, fourth-power scattering law, photomultiplier response, grating response, very slight variations in the laser spot position on changing from *C* to *B*, etc.

The fluorescence intensity, upon changing from the *C* to *B* radiations, is given as

$$I(C,F,\omega + \Delta) = I(B,F,\omega)\eta \quad (2)$$

Here an assumption should be mentioned, namely, that the fluorescence spectrum, when plotted on an *absolute wavenumber* scale, the reciprocal of the wavelength, is invariant in position and shape. (Fluorescence spectra are known whose shapes are wavelength dependent,¹¹ but they are somewhat rare and were not involved in this work. The present method is inapplicable when such wavelength-dependent fluorescences are involved.)

An alternative statement of the above assumption is that the fluorescence spectrum retains its exact shape, but shifts by the wavenumber difference between two different excitations, when it is plotted on a Raman *wavenumber shift* scale. This apparent shift, due to the method of plotting, is illustrated in Figure 1 by the sharp fluorescence doublet of chromium-doped aluminum oxide (ruby).

We next define a decrement function as follows,

$$\delta f(\omega) = I(C,T,\omega) - \eta I(B,T,\omega) \quad (3)$$

where the two intensity terms on the right hand side (RHS) refer to the total intensities excited by the *C* and *B* radiations. Recall that the total intensity is the sum of the fluorescence and Raman intensities.

The two RHS terms of eq 3 may be developed further as follows

$$I(C,T,\omega) = I(C,R,\omega) + I(C,F,\omega) \quad (4)$$

$$\eta I(B,T,\omega) = \eta I(B,R,\omega) + \eta I(B,F,\omega) \quad (5)$$

Substitution of eqs 4 and 5 into eq 3, with further substitution of eqs 1 and 2, leads to the same decrement function as in eq 3, but now the variables are *C*, *F*, and ω ; namely,

$$\delta f(\omega) = I(C,F,\omega) - I(C,F,\omega + \Delta) \quad (6)$$

where Δ refers specifically to $B \rightarrow C$.

Simple reorganization of eq 6 leads to the recursion equations.

The forward recursion equation (FRE) is given as follows,

$$I(C,F,\omega + \Delta) = I(C,F,\omega) - \delta f(\omega) \quad (7)$$

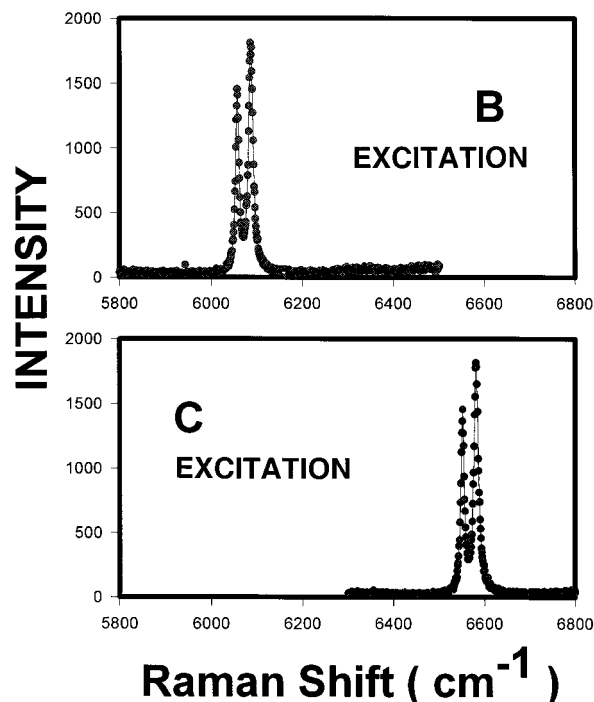


Figure 1. Apparent shift, by 494.6 cm^{-1} , of the ruby fluorescence doublet when excited by the *B* and *C* excitations and plotted on a Raman frequency scale. *B* = 488.0 nm, and *C* = 476.5 nm. No shift would occur if plotting were accomplished on an absolute wavenumber scale.

The backward recursion equation (BRE) is given by

$$I(C,F,\omega) = I(C,F,\omega + \Delta) + \delta f(\omega) \quad (8)$$

The $\delta f(\omega)$ term in eqs 7 and 8 is used in the form shown in eq 3; it is the *scaled* difference between the experimental spectra, that is, the scaled total intensities.

A given calculation involves *exclusive* use of the FRE or of the BRE. One might use the FRE if the high-frequency Raman data contain intense, unremovable plasma lines or the BRE if the low-frequency Raman data are noisy. However, use of both allows for comparisons and for choice of the better result: lower noise level, no artifacts, etc. The FRE and BRE results can also be checked to determine that they are essentially equivalent. The FRE and BRE results should be identical, in the absence of artifacts.

The FRE and BRE are somewhat analogous to differential equations which involve boundary conditions, but the recursion equations involve ω , and thus require *initial conditions*. For example, an initial condition is that $I(*,F,\omega) = 0$, when $\omega = 6000 \text{ cm}^{-1}$, where * might refer, for example, to the *C* excitation.

The η involved in eq 3 also involves some constraints. For example, an unacceptable choice for η might yield positive fluorescence intensity in one region and negative Raman intensities in another. The following conditions are demanded for an acceptable choice of η : $I(*,F,\omega) \geq 0$, plus $I(*,R,\omega) \geq 0$.

The FRE and BRE involve calculation “loops”, i.e., recursion. Consider eq 7 which refers to the FRE, and assume that the *C*-excited fluorescence intensity, $I(C,F,\omega)$, has a low value at, for example, $\omega = 400 \text{ cm}^{-1}$. Subtraction of the 400 cm^{-1} decrement function gives the value of the *C*-excited fluorescence intensity shifted by Δ ($B \rightarrow C$), i.e., at a Raman shift of $400 + \Delta = 894.6 \text{ cm}^{-1}$. Subtraction of the 894.6 cm^{-1} decrement function from this latter intensity value then gives the *C*-excited

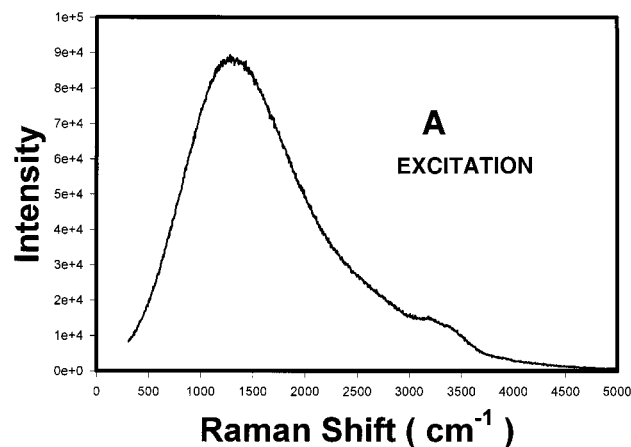


Figure 2. Combined fluorescence and Raman spectra from a red fluorescent dye dissolved in water and excited by the A excitation, 514.5 nm. The peak results from the intense fluorescence, and the minor features between about 3000 and 4000 cm^{-1} refer to the Raman scattering from water. The label e on the ordinate refers to exponent, e.g., $5e+4$, means 5×10^4 , or 50 000 cps. This symbolism is employed when the fluorescence peak count rate exceeds about 40 000 to 50 000 cps.

fluorescence intensity shifted again, namely at 1389.2 cm^{-1} , and so forth. The above procedure can then be repeated for a Raman shift of 401 cm^{-1} , and then 402 cm^{-1} , and so on, at 1 cm^{-1} increments, until the entire, pure fluorescence spectrum is developed.

An analogous procedure may be applied to the BRE, eq 8, when the high-frequency region of the spectrum is of very high quality. In this case the calculation starts at high Raman frequencies and develops the fluorescence spectrum to low frequencies, whereas just the opposite occurs for the FRE.

A key feature of both the BRE and FRE procedures, of course, is the value of η . This value must be obtained by trial and error, but once η has been obtained, the recursion procedure follows directly.

A computer program was developed for use with our recursion equations. This program contains directions for the recursive calculation "loops" which must be carried out by the computer. The computer program is presented in the Appendix, part B.

A succinct mathematical synopsis, which is the basis for the computer program, is presented in part A of the Appendix.

Aqueous Red Dye Illustration

Figures 2–4 depict total fluorescence plus Raman spectra from a fluorescent water-soluble red dye in water.

The predominant part of the total intensity shown in Figures 2–4 arises from a very broad fluorescence. The peak frequency on the Raman shift scale moves upward by an amount equal to $\Delta = 1055.5 \text{ cm}^{-1}$, from A \rightarrow B, i.e., from Figure 2 to Figure 3, and by an amount equal to $\Delta = 494.6 \text{ cm}^{-1}$, from B \rightarrow C, from Figures 3 to 4.

The OH-stretching Raman contour from the water is seen as a weak, structured hump between ≈ 3000 and 3800 cm^{-1} on the broad fluorescence contours shown in the three figures.

A value of $\eta = 1.8$ was determined from the spectra of Figures 2 and 3. A decrement function was then obtained, Figure 5, from the data of Figures 2 and 3. The recursion function was then used to calculate the fluorescence spectrum. This fluorescence spectrum was next used with the Figure 4 data, as depicted in Figure 6.

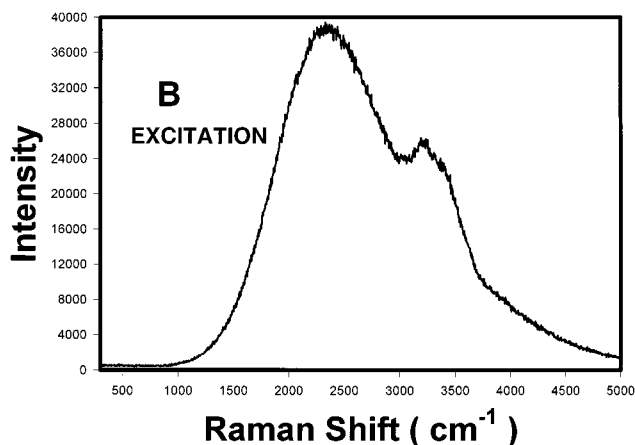


Figure 3. Combined fluorescence and Raman spectra from red fluorescent dye in water, excited by the B excitation, 488.0 nm. See Figure 2 for nature of features.

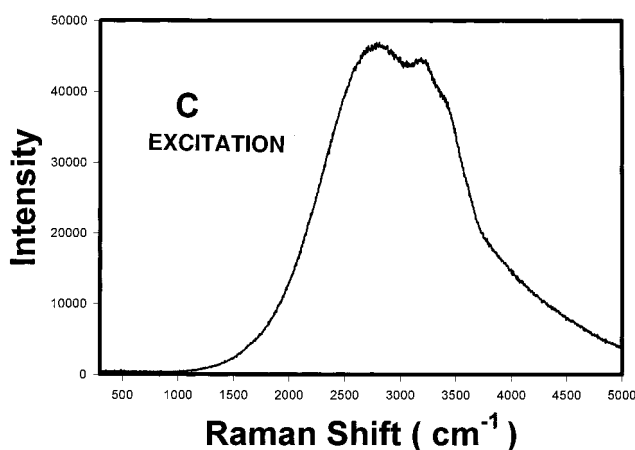


Figure 4. Combined fluorescence and Raman spectra from red fluorescent dye in water, excited by the C excitation, 476.5 nm. See Figure 2 for nature of features.

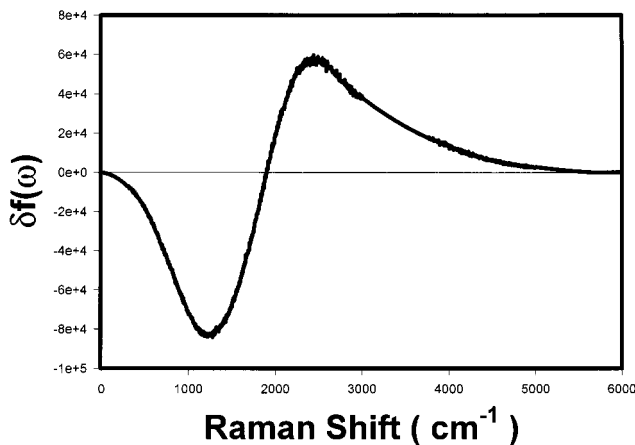


Figure 5. Decrement function, ordinate, plotted versus Raman frequency and obtained from the data of Figures 2 and 3. The symbol, e, on the ordinate refers to exponent, e.g., $8e+4$, means 8×10^4 , or 80 000 cps.

Figure 6 shows the calculated fluorescence spectrum and the total C-excited spectrum above it in the Raman OH-stretching region of water. The difference between the experimental C-excited spectrum and the calculated fluorescence spectrum in the region of about 3000–3800 cm^{-1} is the Raman spectrum of water. The Raman spectrum of water, calculated from the difference, is shown on an expanded scale in Figure 7.

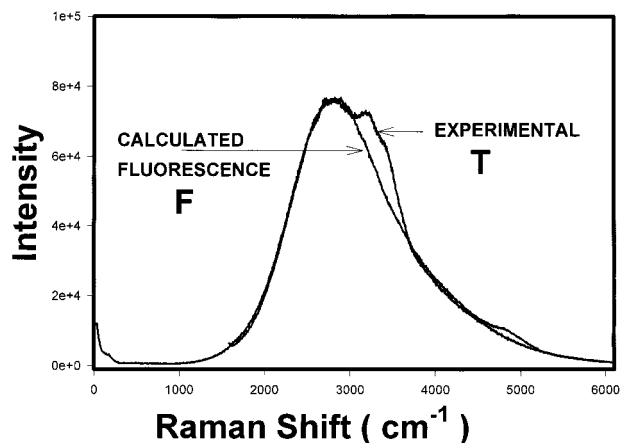


Figure 6. Fluorescence spectrum calculated with the aid of the decrement function determined from the *A* and *B* excitations, compared to the total experimental spectrum, fluorescence plus Raman scattering, obtained with the *C* excitation. The small feature near 5000 cm^{-1} is a mathematical “mirror” artifact and should be ignored.

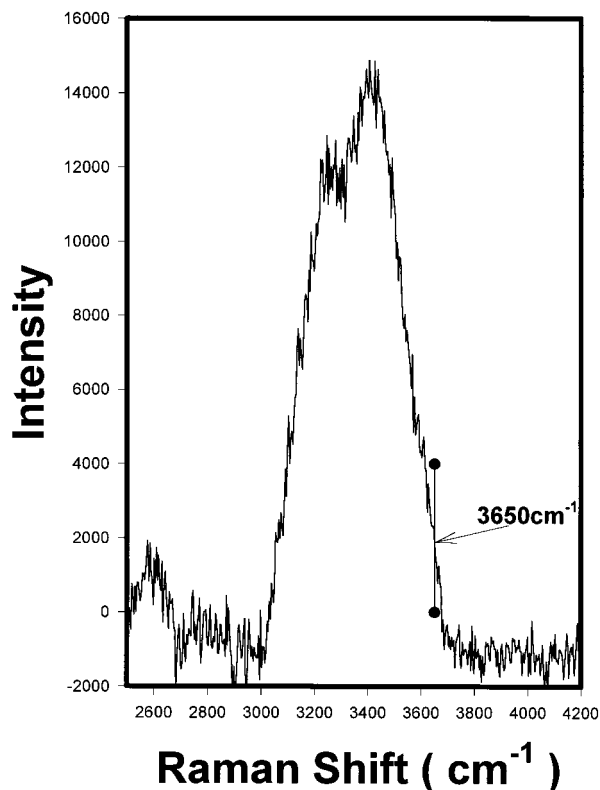


Figure 7. Raman intensity of the water component from the red fluorescent dye solution calculated from the data of Figure 6. Note the small shoulder near 3650 cm^{-1} , filled circles connected by vertical line. This feature arises from OH oscillators which are not hydrogen bonded.

The Raman spectrum of water, Figure 7, shows the key features that any Raman spectrum of pure water displays when obtained with the $X(Z, X + Z)Y$ geometry,¹² namely, a peak at 3400 cm^{-1} and a pronounced low-frequency shoulder at about 3250 cm^{-1} . These two features are visually evident in Figures 2 to 4.

The Figure 7 spectrum also displays a weak high-frequency shoulder (arrow) in the vicinity of 3650 cm^{-1} , which is not evident in Figures 2–4. This 3650 cm^{-1} shoulder is seen in high signal-to-noise ratio Raman spectra from pure water.¹³ The fact that the 3650 cm^{-1} shoulder was uncovered attests to the accuracy and sensitivity of the recursive method.

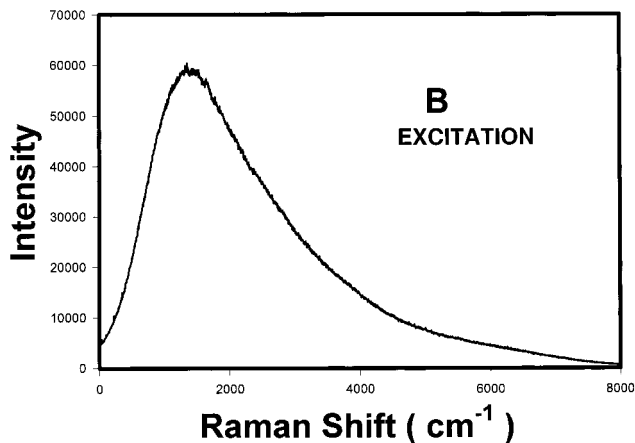


Figure 8. Total fluorescence plus Raman scattering from a solid diamond composite sample excited by the *B* excitation, 488.0 nm .

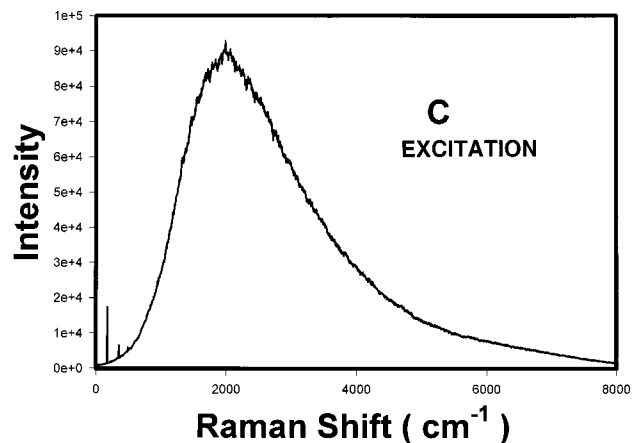


Figure 9. Total fluorescence plus Raman scattering from a solid diamond composite sample excited by the *C* excitation, 476.5 nm .

The argument might be made, of course, that one might simply draw an upwardly curved “base line” on, for example, the Figure 3 spectrum between about 2800 and 3800 cm^{-1} and that the OH-stretching Raman spectrum from water could then be determined by difference. However, this procedure would necessarily involve an assumption about the shape of the base line. The present recursive procedure, in contrast, *does not* involve any such assumptions. We emphasize that the Raman spectrum of water is calculated entirely from experimental data with our recursive method.

The preceding illustrative example involved *three* excitation frequencies. However, it is not necessary to use more than two excitation frequencies. In the following two practical applications, only *two* excitation frequencies are employed.

Recursive Technique Applied to Two Diamond-Composite Samples

Total, i.e., Raman plus fluorescence, spectra from a diamond-composite sample are shown in Figures 8 and 9. Figure 8 was obtained with 488.0 nm , blue 1, *B* excitation, and Figure 9 with 476.5 nm , blue 2, *C* excitation. No visual evidence whatsoever of Raman features is apparent in either figure.

An η value was obtained and, from it, a decrement function, shown in Figure 10. The fluorescence spectrum and the Raman spectrum were then calculated, Figure 11.

Examination of Figure 11 reveals the weakness of the Raman spectrum, compared to the fluorescence spectrum. The peak of the fluorescence spectrum corresponds to $\approx 57\,000\text{ cps}$, whereas the peak of the Raman spectrum is smaller by a factor of ≈ 10 .

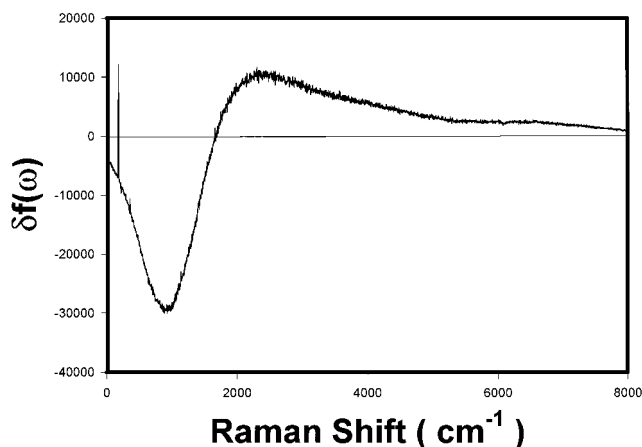


Figure 10. Decrement function, ordinate, plotted on the Raman frequency scale and obtained from the data of Figures 8 and 9.

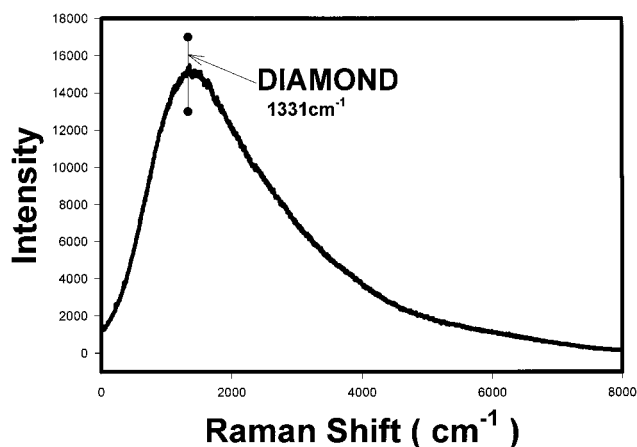


Figure 12. Raman spectrum from the diamond-composite sample calculated recursively using the decrement function. The Raman frequency corresponding to a large crystalline diamond is shown by the filled circles and vertical line. The diamond composite has its Raman peak near that of diamond, but the breadth of the Raman feature is enormous, compared to well-crystallized diamond.

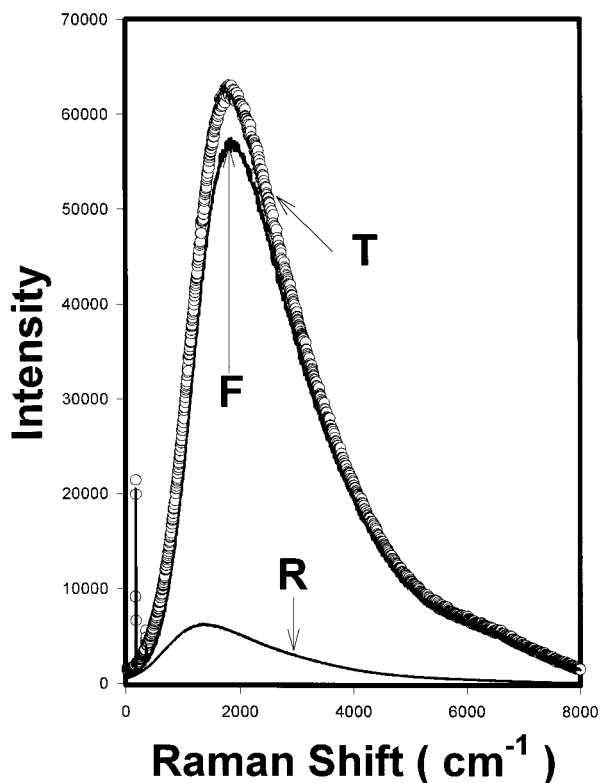


Figure 11. Comparisons between total, *T*, fluorescence, *F*, and Raman, *R*, intensities. The *F* and *R* contributions were obtained by the recursive procedure using the decrement function of Figure 10.

The pure Raman spectrum calculated by the recursion procedure is shown in Figure 12. The peak occurs almost exactly at the 1331 cm^{-1} position of crystalline diamond, highlighted by the two points connected by the vertical bar.

A large, well-crystallized diamond displays an extremely sharp Raman peak at 1331 cm^{-1} .¹⁴ The Raman spectrum from the diamond composite of Figure 12 peaks at the correct position for diamond, but it is very broad and asymmetric. This breadth and asymmetry of the sample is the result of small amounts of graphite (and possibly some hard carbon), plus disorder in all of these constituents. The diamond composite sample has a ceramic-like or glass-like disordered structure resulting from its synthesis at high temperature and high pressure.¹⁵

The question of disorder, however, is not treated here.

X-ray diffraction data were obtained from the diamond-composite sample. The X-ray diffraction pattern displayed

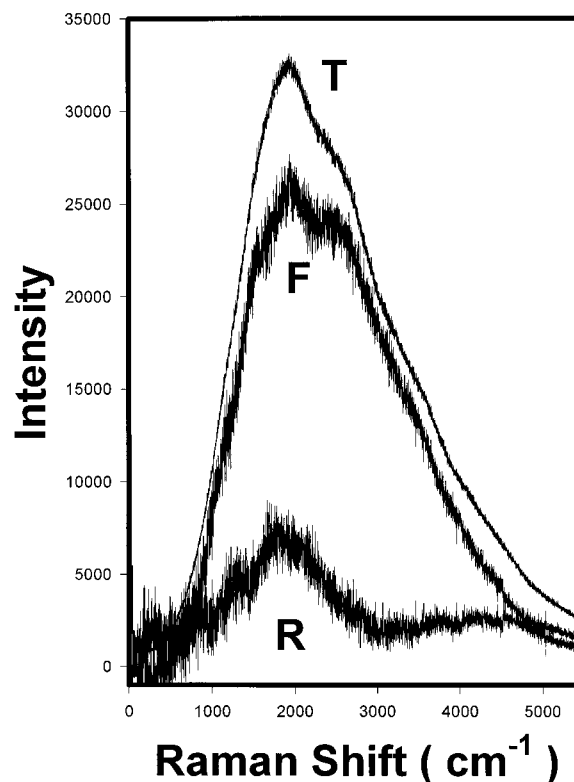


Figure 13. Comparisons between total, *T*, fluorescence, *F*, and Raman intensities, *R*, from a diamond-composite sample composed largely of diamond and graphite. The graphite component gives rise to Raman scattering near the peak of the *R* spectrum, whereas the diamond component produces the shoulder near 1330 cm^{-1} on the *R* spectrum.

extremely high intensities at the diamond positions. An intense line was observed at a 2θ of 43.9° , a line of intermediate intensity at a 2θ of 75.3° , and a weaker line at a 2θ of 91.5° , in agreement with the known lines expected of diamond.¹⁶ An extremely weak line was observed near a 2θ position of 26.38° , a line of graphite. The ratio of the 43.9° diamond to 26.38° graphite intensity was roughly 200, indicating that the diamond to graphite ratio was very high. This agrees with the observation that the predominant Raman intensity of Figure 12 occurs at the diamond position.

TABLE 1: Program:T350.BAS

```

5 DIM DF(10000),FP(10000),RP(10000),P(10000)
10 OPEN "POB.DAT" FOR INPUT AS #1
    ----Input Raman experimental data: 476.5nm data C, SEE Fig 9.
20 OPEN "BOA.DAT" FOR INPUT AS #2
    ----Input Raman experimental data: 488nm data B, SEE Fig 8.
30 OPEN "DF350.DAT" FOR OUTPUT AS #3
    ----Output function DF350.DAT, See Fig 10.
40 OPEN "FP350.DAT" FOR OUTPUT AS #4
    ----Output the solution of the program: Fluorescence data,see Fig 11. As you can
    see, F data are very large.
50 OPEN "RP350.DAT" FOR OUTPUT AS #5
    ----Output the solution of the program: Raman data,
    see Fig 12.As you can see, the material
    is DIAMOND COMPOSITE.
60 OPEN "B&P350.DAT" FOR OUTPUT AS #6
    ----Output the Experimental data ( After, use ETA.).
100 DELTA=496
    ----C and B is shift D=20986 - 20491=495cm-1 but
    need to put in the system experimental error ( 1.0cm-1).
102 ETA=(62397/42857)*0.1
    ---- This is best ETA
110 FOR I=23 TO 7999 STEP 4
112 INPUT#1,X1,P :P(I)=P
114 INPUT#2,X2,B
115 REM PRINT"++++++"X1,X2
116 DF=P-ETA*B :DF(I)=DF
118 PRINT#3,X1,DF
119 PRINT#6,X1,(ETA*B),P
120 NEXT I
    ----DF loop, and output DF ( 30 ), Experimental data ( 60 ).
-----
122 FOR I=7999 TO 9345 STEP 4
124 FP(I)=0
126 NEXT I
    ----Loop for setting the INITIAL CONDITION:
    FP( ω )=0 when ω >8000cm-1.
-----
128 FOR I=7999 TO 23 STEP -4
130 J=I+ 497
132 FP(I)=FP(J)+DF(I)
135 REM PRINT"-----"
136 NEXT I
    ----Loop for the BACKWARD RECURSION EQUATION
    solve the solution FP( ω ). See Equation ( 5 )
-----
140 FOR I=23 TO 7999 STEP 4
141 X=1.0*I
142 PRINT#4,X,FP(I)
144 RP=P(I)-FP(I) :RP(I)=RP
145 IF I<100 THEN PRINT"*****<1>"I,FP(I),RP
146 PRINT#5,X,RP
147 NEXT I
    ---- Loop for the output of the solution FP(ω) and RP(ω).
-----
148 PRINT"*****"
149 INPUT"*****",A$
150 FOR I=3999 TO 4199 STEP 4
152 PRINT"*****<2>"I,FP(I),RP(I)
154 NEXT I
    ---- Loop for testing for best ETA: for all ω, FP>=0, and RP>=0.
    If the condition is not satisfied, then change the ETA ( 102).
-----
156 CLOSE #1,#2,#3,#4,#5,#6
160 PRINT"*****"
200 END

```

A second, entirely different, diamond-composite sample was examined whose X-ray diffraction pattern revealed lines of

graphite (and possibly some hard carbon) plus lines of diamond. The diamond-to-graphite X-ray intensity ratio was much lower than that of the sample, discussed above. This sample was synthesized many months earlier than the sample corresponding to Figure 12, at a time when the conversion to diamond was not so complete.¹⁵ The total, fluorescence, and Raman spectra from this second sample, obtained by the recursive method, are shown in Figure 13.

The Raman spectrum of Figure 13 reveals a shoulder near 1300 cm⁻¹, from diamond, and a peak near 1600–1800 cm⁻¹, from graphite. All Raman features are very broad. This breadth arises from component overlap, e.g., of the diamond and graphite Raman components, and also because of the structural disorder of all of the sample's constituents.

Conclusion

A new dual-excitation method of separating Raman scattering from fluorescence has been developed that involves recursive computations. The necessary recursion equations were derived, and the conditions required for the correct use of the recursion equations were given. The experimental method was also described with one illustrative, three-color, as well as two practical, two-color, examples. The recursive method is applicable to the separation of fluorescence from Raman scattering when the fluorescence is not more than ≈10 times more intense than the Raman scattering. The new method should be of use to practicing Raman spectroscopists.

Acknowledgment. The efforts of L. A. Kabacoff and of G. J. Piermarini in obtaining X-ray scattering data from the diamond-composite samples are greatly appreciated. This work was supported by a contract from the Office of Naval Research.

Appendix

This appendix contains the following: (A) a synopsis of the recursion equations and the constraints imposed upon them, and (B) the computer program necessary for conducting the recursion calculations.

(A) Synopsis of Recursion Procedure. The recursion equations are specified to the *B* and *C* excitations, as an example.

The Raman intensities for the *B* and *C* excitations are related by

$$I(C,R,\omega) = I(B,R,\omega)\eta \quad (\text{A1})$$

The Raman spectral shapes, but not overall intensities, are invariant from *B* to *C*.

The fluorescence intensities for the *B* and *C* excitations are related by

$$I(C,F,\omega) = I(B,F,\omega - \Delta)\eta \quad (\text{A2})$$

The fluorescence shifts between the *B* and *C* excitations by an amount Δ . The fluorescence shapes are assumed to be ω invariant.

We define the decrement function as

$$\delta f(\omega) = I(C,T,\omega) - \eta I(B,T,\omega) \quad (\text{A3})$$

The forward recursion equation which results is

$$I(C,F,\omega + \Delta) = I(C,F,\omega) - \delta f(\omega) \quad (\text{A4})$$

The backward recursion equation which results is

$$I(C,F,\omega) = I(C,F,\omega + \Delta) + \delta f(\omega) \quad (\text{A5})$$

The initial condition corresponds to $\omega < \omega_{\min}$ or to $\omega > \omega_{\max}$. This initial condition is

$$I(*,F,\omega) = 0 \quad (\text{A6})$$

where * refers here to *B* or *C*.

Use the FRE (4) or the BRE (5) and the initial condition (6) in conjunction with the computer program (see B section, program name, T350.BAS). $\delta f(\omega)$ is known from the experimental data. Then use the decrement equation to solve for $I(C,F,\omega)$, and obtain the Raman and fluorescence spectra, individually.

If $\delta f(\omega)$ is preferable (less noisy, fewer artifacts, etc.) at large ω , compared to low ω , choose the BRE, or vice versa.

The best η must satisfy the condition, $I(*,R,\omega) \geq 0$ and $I(*,F,\omega) \geq 0$, where * refers to a given excitation, e.g., *C*. The Raman and fluorescence intensities can never be negative.

B. Computer Program. The computer program, T350.BAS, is given in Table 1.

References and Notes

- (1) Van Duyne, R. P.; Jeanmaire, D. L.; Shriver, D. F. *Anal. Chem.* **1974**, *46*, 213.
- (2) Strommen, D. P.; Nakamoto, K. *Laboratory Raman Spectroscopy*; Wiley: New York, 1984; p 95.
- (3) Schoen, P. E.; Priest, R. G.; Sheridan, J. P.; Schnur, J. M. *Nature* **1977**, *270*, 412. Schoen, P. E.; Schnur, J. M.; Sheridan, J. P. *Appl. Spectrosc.* **1977**, *31*, 337. Schoen, P. E.; Priest, R. G.; Sheridan, J. P.; Schnur, J. M. *J. Chem. Phys.* **1979**, *71*, 317.
- (4) Friedman, J. M.; Hochstrasser, R. M. *Chem. Phys. Lett.* **1975**, *33*, 225. Maroni, V. A.; Cunningham, P. T. *Appl. Spectrosc.* **1973**, *27*, 428.
- (5) Walrafen, G. E. *J. Chem. Phys.* **1970**, *52*, 4176. See page 4177, left column, first paragraph.
- (6) Walrafen, G. E.; Hokmabadi, M. S.; Yang, W.-H.; Chu, Y. C.; Monosmith, B. *J. Chem. Phys.* **1989**, *93*, 2909.
- (7) Blatz, L. A. In *Raman Spectroscopy*; Szymanski, H. A., Ed.; Plenum: New York, 1970; p 123, Vol. 2. Blatz, L. A. *Anal. Chem.* **1961**, *33*, 249. Blatz, L. A.; Waldstein, P. *J. Phys. Chem.* **1968**, *72*, 2614.
- (8) Walrafen, G. E.; Hokmabadi, M. S.; Yang, W.-H. *J. Phys. Chem.* **1988**, *92*, 2433. See page 2434, left column, fourth paragraph.
- (9) Walrafen, G. E.; Yang, W.-H.; Chu, Y. C.; Hokmabadi, M. S. *J. Phys. Chem.* **1966**, *100*, 1381. See page 1382, left column, first paragraph.
- (10) Walrafen, G. E. *J. Chem. Phys.* **1971**, *55*, 768. Figure 15 on page 781 involved treatment of the solution with H₂O₂.
- (11) Walrafen, G. E.; Hokmabadi, M. S.; Chu, Y. C. In *Hydrogen-Bonded Liquids*; Dore, J. C., Teixeira, J., Eds.; Kluwer Academic: Dordrecht, 1991; pp 272, 273. A solution of sucrose in water, saturated at 70 °C, was found to have a frequency-dependent fluorescence shape.
- (12) Walrafen, G. E.; Hokmabadi, M. S.; Yang, W.-H. *J. Chem. Phys.* **1986**, *85*, 6964.
- (13) Walrafen, G. E.; Fisher, M. R.; Hokmabadi, M. S.; Yang, W.-H. *J. Chem. Phys.* **1986**, *85*, 6970.
- (14) Walrafen, G. E.; Chu, Y. C. Unpublished work.
- (15) Kear, B. Private communications.
- (16) Piermarini, G. J. Private communications.